Quantitative structure–activity relationship modeling of S-triazines and 2-arylpyrimidines as selective PDE4B inhibitors

Choo Shiuan Por, Gabriel Akyirem Akowuah, Anand Gaurav

Department of Pharmaceutical Chemistry, Faculty of Pharmaceutical Sciences, UCSI University, No. 1, UCSI Heights, Jalan Menara Gading, Taman Connaught, 56000 Kuala Lumpur, Malaysia

Corresponding author:
Anand Gaurav, Faculty of Pharmaceutical Sciences, UCSI University, No. 1, UCSI Heights, Jalan Menara Gading, Taman Connaught, 56000 Kuala Lumpur, Malaysia.
E-mail: anand.pharma@gmail.com

ABSTRACT

Introduction: A QSAR analysis was performed on a series of 2-arylpyrimidine and s-triazine derivatives as selective PDE4B inhibitors. Primary objective of the study was to develop predictive QSAR models for s-triazines and 2-arylpyrimidines as selective PDE4B inhibitors and to identify structural features which are responsible for the PDE4B selectivity. **Materials and Methods:** A data set comprising 62 compounds as PDE4B inhibitors was used for development of first QSAR model while data set of 57 compounds as PDE4D inhibitors was used to develop another QSAR model. Data set was divided into training (80%) and test (20%) set by using K-mean clustering method. CDK and chemaxon descriptors were obtained for all compounds. QSAR model was built using multiple linear regression (MLR) technique. Squared cross-validation leave one out (LOO) coefficient (R2cv) for internal validation was calculated whereas external validation was performed by predicting the activity of test set using QSAR model developed. **Conclusion:** The results suggest that ATSm4, Wlambda3.unity, C1SP1, RNCS, TPSA, asa_ASA_P_pH_7.4 and maximalprojectionradius are important in determining the PDE4B inhibition, while BCUT-1l, WNSA-3, nAtomP, TPSA and C1SP3 are vital structural features in determining the PDE4D inhibition. TPSA and C1SP3 are negatively correlated with the PDE4D inhibition.

INTRODUCTION

Asthma and chronic obstructive pulmonary disease (COPD) are common inflammatory diseases of lung in general population. Prevalence of asthma and COPD has increased in recent years, with more than 200 million people affected by it worldwide. The drugs mainly used to manage inflammation in COPD and asthma are inhaled glucocorticoids which are combined with β_2-agonists/antimuscarinics to relax the airways.[1] β_2-agonists act on β_2-adrenoceptor, activate adenylyl cyclase, and increase cytosolic cyclic adenosine monophosphate (cAMP) level.[2] Glucocorticoids bind to glucocorticoid receptor (GR) in cytoplasm to form activated GR, which reduces nuclear factor-κB-associated coactivator activity, thus reducing histone acetylation.[2] However, the clinical experience with this particular drug class in COPD and steroid-resistant asthma has been disappointing, and it has been suggested that the lack of efficacy of these drugs in this disease is attributable to a molecular defect in histone deacetylase activity.[3] Glucocorticoids are ineffective in smokers due to oxidation stress, resulting in increased PI3Kδ activation.[4] Recent study found that theophylline, which is a non-selective phosphodiesterase 4 (PDE4) inhibitor, managed to restore histone deacetylase activity and inhibit PI3Kδ.[3,4] Hence, PDE4 inhibitor has been selected to treat COPD and steroid-resistant asthma.

PDE4, a main selective cAMP-metabolizing enzyme in inflammatory and immune cells, includes four subtypes such as PDE4A, PDE4B, PDE4C, and PDE4D. Many PDE4 inhibitors in development are efficacious in animal models of various inflammatory disorders such as asthma, COPD, psoriasis, inflammatory bowel diseases, and rheumatoid arthritis[5] as well as in clinical trials for asthma and COPD.[6] The treatments for respiratory disorders with PDE4 inhibitors are not definitive due to narrow therapeutic window of most of the compounds.[7] A major reason for their poor clinical results is the consequence of dosing limitation when administered orally and lack of sufficient activity when inhaled and the side effects such as nausea and emesis, which make it intolerable

in some patients.[8] Studies have shown that inhibition of PDE4D has been associated with nausea and vomiting.[9] A recent study has shown that deletion of PDE4D and not PDE4B reduced the duration of anesthesia-induced xylazine in mice, where the xylazine was used as a replacement of emesis since rodents do not possess an emetic reflex.[10] more importantly, recent findings in PDE4 knockout mice suggest that an inhibitor with PDE4B selectivity should retain many beneficial anti-inflammatory effects without the unwanted side effects.[11] Thus, selective PDE4B inhibitors are valid, promising therapeutic intervention for different inflammatory conditions including those of respiratory tract like asthma.

Several lead compounds with diverse structures have been identified as selective PDE4B inhibitors. 1,3,5-triazines (s-triazines) and 2-arylpyrimidines are among the most promising categories of selective PDE4B inhibitors discovered recently. The compounds belonging to these categories have demonstrated more than 100-fold selectivity for PDE4B versus PDE4D.[11a,12] The optimization of these compounds can further improve the selectivity for PDE4B.

In silico studies, i.e., quantitative structure–activity relationship (QSAR) and other ligand-based drug design techniques have widely been used in the past to optimize activity of lead compounds and identify structural requirement of receptors.[13] Thus, this study has been designed to use QSAR to develop predictive QSAR models for s-triazines and 2-arylpyrimidines and identify the structural features of s-triazines and 2-arylpyrimidines responsible for their PDE4B selectivity.

MATERIALS AND METHODS

Data Sets

A data set comprising 62 compounds as PDE4B inhibitors was used for the development of first QSAR model while data set of 57 compounds as PDE4D inhibitors was used to develop another QSAR model. The compounds included 2-arylpyridine derivatives and s-triazine derivatives. The compounds and their IC_{50} values were collected from the literature [Table 1].[11a,12] IC_{50} values were converted to pIC_{50} ($-\log IC_{50}$) for the development of QSAR model.

Data set was divided into training (80%) and test (20%) set using K-mean clustering method. For the PDE4B inhibitors, data set was split into training set containing 50 molecules and test set containing 12 molecules [Table 2]. For PDE4D inhibitors, data set was divided into training set containing 46 molecules and test set containing 11 molecules Table 2.

Calculation of Descriptors

ACD/ChemSketch 2016.1 was used to draw the structures of compounds in the training set and the test set.[14] All structures were uploaded to Online Chemical Database (https://ochem.eu/descriptorscalculator/show.do) for calculation of descriptors.[14,15] All structures were processed using Chemaxon Standardizer.[15,16] Standardization was applied to transform all molecules according to a set of SMARTS templates. All molecules were neutralized and salts were removed. Clean structure was applied to remove 3D or atom coordinate calculation information and prevent model overfitting.[16] All

the structures were converted to 3D and optimized by Corina before calculation of descriptors.[15]

A number of CDK descriptors were calculated such as constitutional descriptors, geometric descriptors, hybrid descriptor, topological descriptors, and electronic descriptors. Chemaxon descriptors such as elemental analysis, charge, geometry, partitioning, protonation, and isomers for pH 7.4 were calculated for every molecule. pH 7.4 was used for the calculation of Chemaxon descriptors.

QSAR Modeling

QSAR model was built using multiple linear regression (MLR) technique. The descriptors were used on the independent variables whereas the pIC_{50} values were used on the dependent variables. MATLAB® R2016b software was used to build the QSAR equation with best regression equation (highest correlation of determination, R^2) value using stepwise regression.[17] Descriptors were added one by one into the equation to determine which final combination of descriptors gives the best R^2. All descriptors included in the QSAR model for PDE4B and PDE4D inhibition were statistically significant ($P < 0.05$). Standard residual, which is the standardized difference of predicted and observed activity value of each molecule, was determined using StatSoft® STATISTICA (trial version) and compound with the highest value of standard residual were considered as outlier.[18] Outliers were deleted to improve the regression's correlation of determination. Correlation of determination (R^2) above or equal to 0.6 suggests a good MLR model.[19] Combination of descriptors obtained was imported into StatSoft® STATISTICA software for determination of R^2 (correlation of determination), R^2_{adj} (adjusted correlation of determination), F (Fisher statistical significance criteria) values, and SE (standard error of estimation). F value indicated overall significance of the model.[19]

Cross-Validation

Cross-validation consists of internal and external validation. Reliability and applicability of the model are examined using cross-validation procedure.

Squared cross-validation leave one out coefficient (R^2 cv) for internal validation was calculated using MATLAB® R2016b software.[17] It involved removal of molecule one by one from the data set, develop the model again, and calculate for Q^2 (cross-validated R^2). For a good predictivity model, Q^2 has to be >0.5, and R^2-Q^2 should not exceed 0.3.[19,20]

External validation was performed by predicting the activity of test set using QSAR model developed. The predicted activities of the molecules in test set were correlated with the observed activities to obtain the R^2_{pred}. Outliers with high standard residual values were deleted from test set. If R^2 for external test set, $R^2_{pred} > 0.6$, the external predictivity of the model was considered as good.[19]

RESULTS AND DISCUSSION

QSAR Model for PDE4B Inhibition

QSAR model was generated for PDE4B inhibition using combination of CDK and Chemaxon descriptors. Stepwise
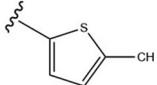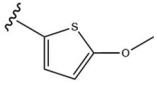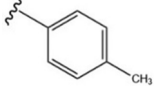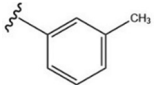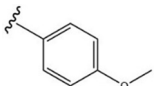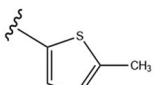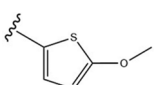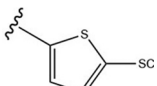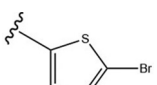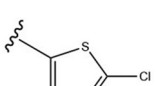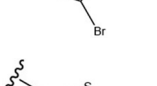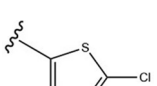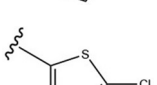
Table 1: Structures and activity of 2-arylpyridine derivatives as PDE4B and PDE4D inhibitors[11a,12]
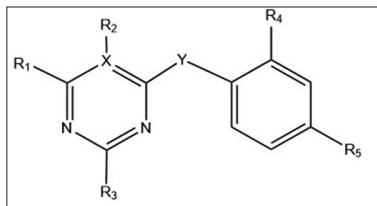
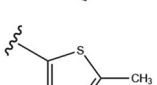| Entry	R^1	R^2	R^3	R^4	R^5	X	Y	PDE4B IC$_{50}$ (nM)	PDE4D IC$_{50}$ (nM)
1	Me	–CH$_2$CH=CH$_2$	Ph	H	–COOH	C	NH	190	1900
2	Me	Me	Ph	H	–COOH	C	NH	430	3400
3	Me	Et	Ph	H	–COOH	C	NH	140	2100
4	Me	*n*-Pr	Ph	H	–COOH	C	NH	1300	7600
5	Me	–CN	Ph	H	–COOH	C	NH	120	1500
6	Me	–CHO	Ph	H	–COOH	C	NH	300	1500
7	Me	–CH$_2$OH	Ph	H	–COOH	C	NH	540	8000
8	Et	–CH$_2$CH=CH$_2$	Ph	H	–COOH	C	NH	34	82
9	*n*-Pr	–CH$_2$CH=CH$_2$	Ph	H	–COOH	C	NH	690	2400
10	Me	–CH$_2$CH=CH$_2$		H	–COOH	C	NH	120	1300
11	Me	–CH$_2$CH=CH$_2$		H	–COOH	C	NH	68	990
12	Me	–CH$_2$CH=CH$_2$		H	–COOH	C	NH	2800	12000
13	Me	–CH$_2$CH=CH$_2$		H	–COOH	C	NH	3700	15000
14	Me	–CH$_2$CH=CH$_2$		H	–COOH	C	NH	860	3000
15	Me	–CH$_2$CH=CH$_2$		H	–COOH	C	NH	220	2800
16	Me	–CH$_2$CH=CH2		H	–COOH	C	NH	210	1500
17	Me	–CH2CH=CH2		H	–COOH	C	NH	220	2000
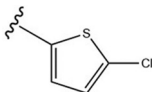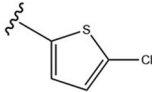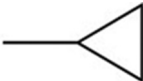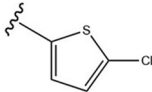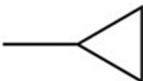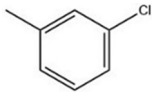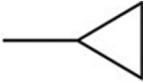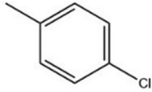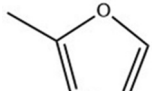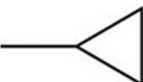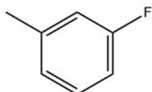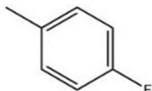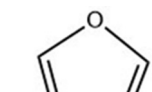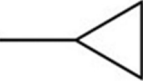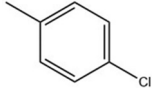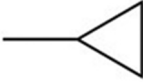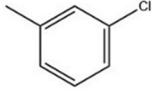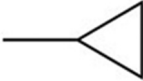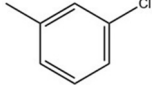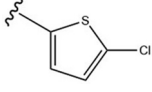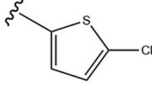
(Contd...)

Table 1: *(Continued)*

Entry	R^1	R^2	R^3	R^4	R^5	X	Y	PDE4B IC$_{50}$ (nM)	PDE4D IC$_{50}$ (nM)
18	Me	–CH$_2$CH=CH$_2$		H	–COOH	C	NH	150	1300
19	Me	–CH$_2$CH=CH$_2$		H	–COOH	C	NH	78	760
20	Me	–CH$_2$CH=CH$_2$	Ph	H	–CH$_2$COOH	C	NH	1800	>10,000
21	Me	–CH$_2$CH=CH$_2$		H	–CH$_2$COOH	C	NH	940	11000
22	Me	–CH$_2$CH=CH$_2$		H	–CH$_2$COOH	C	NH	1200	9900
23	Me	–CH$_2$CH=CH2		H	–CH$_2$COOH	C	NH	600	4800
24	Me	–CH$_2$CH=CH$_2$		H	–CH$_2$COOH	C	NH	320	8800
25	Me	–CH$_2$CH=CH2		H	–CH2COOH	C	NH	190	5300
26	Me	Et		H	–CH$_2$COOH	C	NH	34	1500
27	Me	Et		H	–CH$_2$COOH	C	NH	19	1600
28	Me	Et		H	–CH$_2$COOH	C	NH	15	1700
29	Me	Et		H	–CH$_2$COOH	C	NH	6.8	2900
30	Me	Et		F	–CH$_2$COOH	C	NH	15	3100
31	–OCH$_2$CH$_3$	-	–OCH2CH3	H	–OCH3	N	NH	6700	2300
32	Me	-		H	–CH$_2$COOH	N	NH	1287	NA
33	*i*-Pr	-		H	–CH$_2$COOH	N	NH	1945	3580
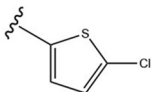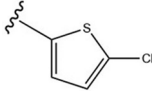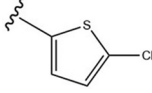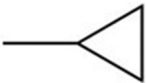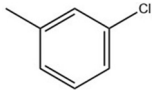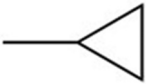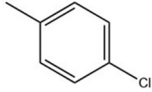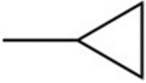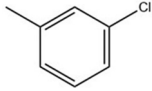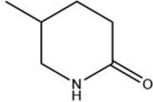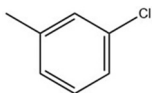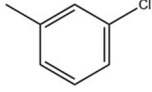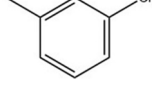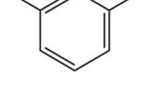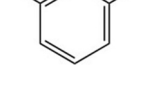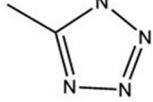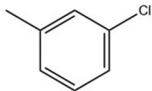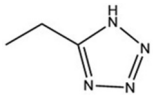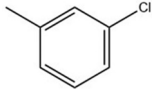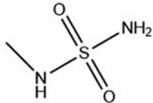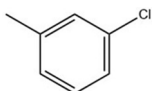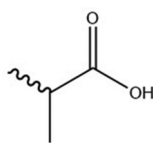
(Contd...)

Table 1: *(Continued)*

Entry	R^1	R^2	R^3	R^4	R^5	X	Y	PDE4B IC$_{50}$ (nM)	PDE4D IC$_{50}$ (nM)
34	Et	-		H	–CH$_2$COOH	N	NH	383	865
35	*n*-Pr	-		H	–CH$_2$COOH	N	NH	2447	NA
36		-		H	–CH$_2$COOH	N	NH	251	1489
37		-		H	–CH$_2$COOH	N	NH	237	1181
38		-		H	–CH$_2$COOH	N	NH	3770	5611
39	Me	-		H	–CH$_2$COOH	N	NH	18755	22260
40		-		H	–CH$_2$COOH	N	NH	1437	2107
41	Et	-		H	–CH$_2$COOH	N	NH	1460	727
42	Et	-		H	–CH$_2$COOH	N	NH	2777	NA
43		-		H	–CH$_2$COOH	N	NHCH$_2$	2282	859
44		-		H	–CH$_2$COOH	N	NHCH$_2$	845	726
45		-		H	–CH$_2$COOH	N	O	1862	2268
46	Me	-		H	–COOH	N	NH	4048	NA
47	Et	-		H	–COOH	N	NH	261	251
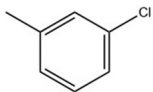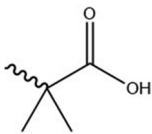
(Contd...)

Table 1: *(Continued)*

Entry	R^1	R^2	R^3	R^4	R^5	X	Y	PDE4B IC$_{50}$ (nM)	PDE4D IC$_{50}$ (nM)
48	Et	-	thiophene-Cl	H	–F	N	NH	1394	207
49	*i*-Pr	-	thiophene-Cl	H	–COOH	N	NH	220	219
50	*i*-Pr	-	thiophene-Cl	H	–F	N	NH	8815	886
51	cyclopropyl	-	phenyl-Cl	H	–COOH	N	NH	46	20
52	cyclopropyl	-	phenyl-Cl	H	–COOH	N	NH	135	268
53	cyclopropyl	-	phenyl-Cl	H	piperidinone	N	NH	135	268
54	Me	-	phenyl-Cl	H	–CH$_2$COOH	N	NH	781	681
55	Me	-	phenyl-Cl	H	–COOH	N	NH	241	213
56	Me	-	phenyl-Cl	H	CN	N	NH	12	13
57	Me	-	phenyl-Cl	H	CH$_2$CN	N	NH	165	7
58	Me	-	phenyl-Cl	H	methyltetrazole	N	NH	126	132
59	Me	-	phenyl-Cl	H	ethyltetrazole	N	NH	69	63
60	Me	-	phenyl-Cl	H	sulfamide	N	NH	402	160
61	Me	-	phenyl-Cl	H	propanoic acid	N	NH	1090	96

(Contd...)

Table 1: *(Continued)*

Entry	R^1	R^2	R^3	R^4	R^5	X	Y	PDE4B IC$_{50}$ (nM)	PDE4D IC$_{50}$ (nM)
62	Me	-		H		N	NH	1574	600

NA: Not available, PDE4D: Phosphodiesterase 4D, PDE4B: Phosphodiesterase 4B

regression was used to determine optimum number of descriptors in modeling of PDE4B QSAR model. The final equation was evaluated by its Q^2 and R^2_{pred} values for its validity and applicability.

The best one-variable model

The best one-variable model contains ATSm4 as correlating descriptor. The model is shown below (Equation 1):

$$pIC_{50}=0.0671\ (\pm0.0159)\ (ATSm4)+3.3075\ (\pm0.7402) \tag{1}$$

$n = 50$, $R^2 = 0.2702$, $R^2_{adj} = 0.2551$, SE = 0.6551, and F = 17.7790

The best two-variable model

Second model shows an appreciable improvement in the statistic. The best two-variable model is shown below (Equation 2):

$$pIC_{50}=0.0688\ (\pm0.0159)\ (ATSm4)-0.1124\ (\pm0.0314)\ (Wlambda3.unity)+3.3075\ (\pm0.7402) \tag{2}$$

$n = 50$, $R^2 = 0.4269$, $R^2_{adj} = 0.4025$, SE = 0.5867, F = 17.5040

The best three-variable model

Further addition of C1SP1 into Equation (2) led to the three-variable model. The model is shown below (Equation 3):

$$pIC_{50}=0.0749\ (\pm0.0135)\ (ATSm4)-0.0971\ (\pm0.0298)\ (Wlambda3.unity)+0.9518\ (\pm0.3357)\ (C1SP1)+4.1845\ (\pm0.7442) \tag{3}$$

$n = 50$, $R^2 = 0.5121$, $R^2_{adj} = 0.4803$, SE = 0.5472, F = 16.0970

The best four-variable model

Fourth model contains four variables, which was formed by adding relative negative charge surface area (RNCS) descriptor into Equation 3. The model is shown below (Equation 4):

$$pIC_{50}=0.0719\ (\pm0.0127)\ (ATSm4)-0.1145\ (\pm0.0288)\ (Wlambda3.unity)+1.2021\ (\pm0.3307)\ (C1SP1)+0.0791\ (\pm0.0304)\ (RNCS)+4.0691\ (\pm0.7029) \tag{4}$$

$n = 50$, $R^2 = 0.5759$, $R^2_{adj} = 0.5382$, SE = 0.5158, F = 15.2780

The best five-variable model

Total polar surface area (TPSA) descriptor was added as contributing variable to Equation 4 to form new equation with better statistical parameters. The best five-variable model is shown below (Equation 5):

$$pIC_{50}=0.0624\ (\pm0.0125)\ (ATSm4)-0.1180\ (\pm0.0271)\ (Wlambda3.unity)+1.3650\ (\pm0.3168)\ (C1SP1)+0.1670\ (\pm0.0439)\ (RNCS)-0.0057\ (\pm0.0022)\ (TPSA)+4.82635\ (\pm0.719974) \tag{5}$$

$n = 50$, $R^2 = 0.6340$, $R^2_{adj} = 0.5924$, SE = 0.4846, F = 15.2410

The best six-variable model

Stepwise regression further led to six-variable model with slight improvement on statistical parameters. The best six-variable model is shown below (Equation 6):

$$pIC_{50}=0.0651\ (\pm0.0121)\ (ATSm4)-0.1267\ (\pm0.0265)\ (Wlambda3.unity)+1.5710\ (\pm0.3210)\ (C1SP1)+0.2059\ (\pm0.0462)\ (RNCS)-0.0081\ (\pm0.0024)\ (TPSA)+0.0086\ (\pm0.0041)\ (asa\_ASA\_P\_pH\_7.4)+3.9905\ (\pm0.8014) \tag{6}$$

$n = 50$, $R^2 = 0.6676$, $R^2_{adj} = 0.6212$, SE = 0.4672, $F = 14.3920$

The best seven-variable model

Addition of maximal projection radius descriptor to Equation (6) resulted in new equation with better statistical parameter. The seven-variable model is shown below (Equation 7):

$$pIC_{50}=0.0616\ (\pm0.0118)\ (ATSm4)-0.2787\ (\pm0.0768)\ (Wlambda3.unity)+1.5997\ (\pm0.3093)\ (C1SP1)+0.2172\ (\pm0.0448)\ (RNCS)-0.0084\ (\pm0.0023)\ (TPSA)+0.0085\ (\pm0.0040)\ (asa\_ASA\_P\_pH\_7.4)+0.7175\ (\pm0.3422)\ (maximalprojectionradius)+0.4669\ (\pm1.8489) \tag{7}$$

$n = 50$, $R^2 = 0.6994$, $R^2_{adj} = 0.6489$, SE = 0.4497, $F = 13.9390$

Addition of further descriptors did not improve the statistical parameters significantly, thus Equation 7 was selected as the optimum model. Analysis of residuals led to identification of molecule entry 13 as outlier. Thus, entry 13 was deleted from the training set to improve the regression. The best seven-variable model is shown below (Equation 8), and the statistical parameters, correlation matrix of descriptors, and the actual and predicted activity are shown in Tables 3-5, respectively.

$$pIC_{50}=0.0611\ (\pm0.0114)\ (ATSm4)-0.2858\ (\pm0.0742)\ (Wlambda3.unity)+1.5312\ (\pm0.3004)\ (C1SP1)+0.2068\ \pm0.0436\ (RNCS)-0.0079\ (\pm0.0022)\ (TPSA)+0.0083\ (\pm0.0038)\ (asa\_ASA\_P\_pH\_7.4)+0.7140\ (\pm0.3303)\ (maximalprojectionradius)+0.4669\ (\pm1.8490) \tag{8}$$

$n = 49$, $R^2 = 0.7166$, $R^2_{adj} = 0.6683$, SE = 0.4341, $F = 14.8140$

Table 2: Training and test sets for PDE4B and PDE4D QSAR model

Table 2: *(Continued)*

Entry	PDE4B dataset	PDE4D dataset
1	Training	Training
2	Training	Test
3	Training	Test
4	Test	Training
5	Training	Training
6	Training	Training
7	Test	Test
8	Training	Training
9	Training	Training
10	Test	Training
11	Training	Training
12	Training	Test
13	Training	Training
14	Training	Training
15	Training	Training
16	Training	Test
17	Test	Training
18	Training	Training
19	Training	Training
20	Training	-
21	Training	Training
22	Training	Training
23	Training	Training
24	Training	Test
25	Training	Training
26	Training	Test
27	Training	Training
28	Training	Training
29	Training	Training
30	Test	Training
31	Test	Test
32	Training	-
33	Training	Training
34	Test	Training
35	Training	-
36	Training	Training
37	Training	Training
38	Test	Training
39	Training	Training
40	Training	Training
41	Training	Training
42	Training	-
43	Training	Test
44	Test	Training
45	Training	Training
46	Training	-
47	Training	Training
48	Training	Training
49	Training	Training
50	Training	Training
51	Training	Training
52	Test	Training
53	Training	Training
54	Training	Training
55	Test	Training
56	Training	Training
57	Training	Training
58	Training	Training
59	Test	Training
60	Training	Test
61	Training	Test
62	Training	Training

(Contd...)

-: Means the entry is not included in dataset, PDE4D: Phosphodiesterase 4D, PDE4B: Phosphodiesterase 4B, QSAR: Quantitative structure–activity relationship

QSAR Equation 8 has a coefficient of determination of 0.7166 (higher than 0.6) which indicates a good correlation between descriptors and the PDE4B inhibitory activity [Figure 1]. Q^2 of 0.5589 and R^2_{pred} of 0.7645 shows good predictivity and applicability of this model. Contributing descriptors of this equation are ATSm4 (Moreau-Broto autocorrelation descriptors using atomic weight), Wlambda3.unity (holistic descriptor introduced by R. Todeschini), C1SP1 (carbon connectivity in terms of hybridization), RNCS, TPSA, asa_ASA_P_pH_7.4 (water accessible surface area of all polar atoms at pH7.4), and maximal projection radius.

ATSm4 is the mean of the products of atomic weight of atoms separated by topological diameter of three atoms.[21] The higher the atomic weight of atoms spaced by topological diameter of three atoms, the higher the ATSm4 value. ATSm4 has a positive correlation with pIC_{50}. Hence, high ATSm4 value is favorable for PDE4B inhibitory activity. Entry 29 has one methyl group and one bromine atom on the thiophenyl ring at position R_3 of compound whereas entry 28 has only one chlorine atom substituent on thiophenyl ring at R_3. Hence, entry 28 has lower PDE4B inhibitory activity than entry 29 because atomic weight of chlorine is lower than bromine atom and there are extra methyl groups on the thiophenyl substituent in entry 29.

Wlambda3.unity is one of the weighted holistic invariant molecular (WHIM) descriptors descriptors introduced by R. Todeschini. Wlambda3.unity is related to molecular size along a principle axis.[22] WHIM descriptors overcome common problems in traditional QSAR approaches, i.e. requirement of a

common molecular reference, a poor conformational approach, and a lack of a global view of the molecules.[23] Negative coefficient of Wlambda3.unity shows inverse relationship of the descriptor with the inhibitory activity (pIC$_{50}$).

C1SP1 indicates triply bound carbon atoms which are bound to one other carbon atom (C≡C−X or X≡C−C, in which X is not carbon atom). Positive coefficient of C1SP1 shows that the compound with more C1SP1 carbon atoms has better PDE4B inhibitory activity. Entry 5, 56, and 57 have one C1SP1 carbon atom within their structure and their IC$_{50}$ value is lower than 200 nM. The PDE4B inhibitory activities of these three compounds are generally higher than those without C1SP1 carbon atoms.
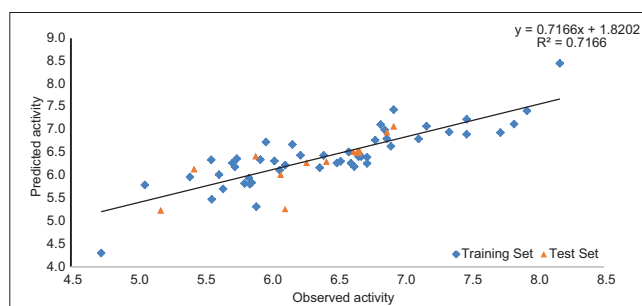
Figure 1: Predicted versus observed activity of Model 8

Table 3: Summary of statistical parameters of QSAR models for PDE4B inhibition

Model No.	R^2	R^2_{adj}	SE	F
Equation 1	0.2702	0.2551	0.6551	17.7790
Equation 2	0.4269	0.4025	0.5867	17.5040
Equation 3	0.5121	0.4803	0.5472	16.0970
Equation 4	0.5759	0.5382	0.5158	15.2780
Equation 5	0.6340	0.5924	0.4846	15.2410
Equation 6	0.6677	0.6212	0.4672	14.3920
Equation 7	0.6991	0.6489	0.4497	13.9390
Equation 8	0.7166	0.6683	0.4341	14.8140

PDE4B: Phosphodiesterase 4B, QSAR: Quantitative structure–activity relationship, SE:Standard error

The next contributing descriptor is RNCS (relative negative charge surface area) of the compound. Formula used for calculation of RNCS is shown below (Equations 15 and 16):

$$RNCS = \frac{\text{Surface area of most negative atom}}{\text{Relative negative charge}} \quad (15)$$

$$\text{Relative negative charge} = \frac{\text{Maximum atomic negative charge in the molecule}}{\text{Negative atomic charge in the molecule}} \quad (16)$$

RNCS has a positive correlation with the inhibitory activity of compound. From Equation 15, surface area and atomic size of most negative atom are proportional to the inhibitory activity of compound. The bigger the most negative atom, the more favorable it is for the PDE4B inhibitory activity. Relative negative charge is the numerator of the Equation 15. It has inverse relation with RNCS. Therefore, the smaller the relative negative charge of the compound, the larger the RNCS. The most negative atom with low negative charge and very large surface area within the compound is favorable for PDE4B inhibitory activity. Molecular structure of entry 49 and 50 differs only at substituent on R$_5$. The most negative atom in entry 50 is fluorine atom, whereas the most negative atom in entry 49 is oxygen atom in carboxyl group. Replacement of carboxyl group containing larger oxygen atom with fluorine atom as in entry 50 results in significant decrease in PDE4B inhibitory activity. Hence, it can be deduced that large surface area of the most negative atom within the compound has a beneficial effect on its PDE4B inhibitory activity.

TPSA is the topological polar surface area of the molecule. It is the sum of the surface area of polar atoms such as oxygen, nitrogen, and their attached hydrogen in the molecule.[24] It plays a role in the prediction of the intestinal absorption of molecule and blood–brain barrier penetration of the molecule.[25] From Equation 8, TPSA has inverse relationship with the inhibitory activity. This indicates that the small surface area of polar atoms such as N and O in the compound is beneficial for PDE4B inhibitory activity. However, there are some limitations of the TPSA descriptor. The TPSA value does not account for influence of positional change of polar fragment.[24] Position of the

Table 4: Correlation matrix of descriptors present in the best QSAR model 8

Parameter	pIC$_{50}$	ATSm4	Wlambda3. unity	C1SP1	RNCS	TPSA	asa_ASA_P_pH7.4	maximalprojectionradius
pIC$_{50}$	1.0000							
ATSm4	0.5206	1.0000						
Wlambda3.unity	−0.4233	0.0260	1.0000					
C1SP1	0.2684	−0.1631	−0.1931	1.0000				
RNCS	0.1019	0.1338	0.2673	−0.3432	1.0000			
TPSA	−0.1106	−0.1049	0.1656	−0.1019	0.7347	1.0000		
asa_ASA_P_pH7.4	−0.1793	−0.2040	0.1414	−0.1687	0.0316	0.3254	1.0000	
Maximal projection radius	−0.3364	0.0632	0.9452	−0.1887	0.2243	0.1418	0.1410	1.0000

QSAR: Quantitative structure–activity relationship

Table 5: Observed and predicted activities along with the residual obtained using QSAR model 8

Entry	Observed value	Predicted value	Residual
1	6.7212	6.3988	0.3225
2	6.3665	6.1700	0.1965
3	6.8539	6.9968	−0.1429
4	5.8861	6.4238	−0.5378
5	6.9208	7.4387	−0.5179
6	6.5229	6.3099	0.2130
7	6.2676	6.2799	−0.0123
8	7.4685	6.9004	0.5682
9	6.1612	6.6771	−0.5160
10	6.9208	−7.0764	−0.1556
11	7.1675	7.0778	0.0897
12	5.5528	6.3409	−0.7881
14	6.0655	6.1158	−0.0503
15	6.6576	6.4494	0.2081
16	6.6778	6.4143	0.2634
17	6.6576	−6.5226	0.1350
18	6.8239	7.1126	−0.2887
19	7.1079	6.7998	0.3081
20	5.7447	6.3673	−0.6225
21	6.0269	6.3162	−0.2893
22	5.9208	6.3454	−0.4245
23	6.2218	6.4426	−0.2207
24	6.4949	6.2720	0.2228
25	6.7212	6.2639	0.4573
26	7.4685	7.2299	0.2386
27	7.7212	6.9384	0.7828
28	7.8239	7.1233	0.7006
29	8.1675	8.4517	−0.2842
31	5.1739	5.2389	−0.0650
32	5.8904	5.3169	0.5736
33	5.7111	6.2710	−0.5599
34	6.4168	6.3044	0.1124
35	5.6114	6.0172	−0.4059
36	6.6003	6.2686	0.3317
37	6.6253	6.1933	0.4319
38	5.4237	6.1392	−0.7156
39	4.7269	4.3029	0.4240
40	5.8425	5.8086	0.0340
41	5.8356	5.9448	−0.1092
42	5.5564	5.4783	0.0781
43	5.6417	5.7053	−0.0637
44	6.0731	6.0195	0.0536
45	5.7300	6.1869	−0.4569
46	5.3928	5.9664	−0.5737

(Contd...)

Table 5: *(Continued)*

Entry	Observed value	Predicted value	Residual
47	6.5834	6.5131	0.0702
48	5.8557	5.8423	0.0135
49	6.6576	6.4142	0.2434
50	5.0548	5.7917	−0.7369
51	7.3372	6.9500	0.3873
52	6.8697	6.9500	−0.0804
53	6.8697	6.8045	0.0651
54	6.1073	6.2265	−0.1191
55	6.6180	6.5146	0.1034
56	7.9208	7.4140	0.5069
57	6.7825	6.7715	0.0110
58	6.8996	6.6391	0.2605
60	6.3958	6.4382	−0.0424
61	5.9626	6.7302	−0.7676
62	5.8030	5.8255	−0.0225

Entry 13 was identified as outlier and was deleted from training set whereas entry 30 and 59 were identified as outliers and deleted from test set

same polar group on a different position, i.e., ortho, meta, or para of benzene ring may contribute to the same TPSA value.[24] TPSA value calculated for entry 6 is higher than entry 2 due to the presence of polar aldehyde group at R_2 position of entry 6 instead of non-polar methyl group at R_2 position of entry 3. Due to inverse relationship of TPSA and PED4B inhibitory activity, entry 6 has lower pIC_{50} than entry 2. Coefficient of TPSA descriptor is lower than other six descriptors in the equation. Hence, it has the lowest contribution to the PDE4B inhibitory compared to other descriptors in the equation.

Asa_ASA_P_pH7.4 is water accessible surface area for all polar atoms ($|q_i| \geq 0.2$) at pH7.4. Value of q_i indicates the point charge of atom located at position i of compound.[21] Only atom with charge more than or equal to 0.2 statcoulomb is taken into account and surface area of such atoms is measured. Positive coefficient of this descriptor indicates that increase in magnitude of asa_ASA_P of compound at pH7.4 will increase its PDE4B inhibitory activity. Generally, the larger the size of polar groups, the larger the surface area of polar group accessible to water.

The last descriptor is maximal projection radius of the compound. It is the radius of maximum projection area of conformer. The geometry and energy of all molecules were optimized before measurement of the maximal projection radius. From Equation 8, maximal projection radius of compound is proportional to its PDE4B inhibitory activity (pIC_{50}). It has the second highest contribution among all descriptors to the PDE4B inhibitory activity.

QSAR Model for PDE4D Inhibition

QSAR model was generated for PDE4D inhibition using combination of CDK and Chemaxon descriptors. Five descriptors were identified as best correlating descriptors with inhibitory activity of compounds.

The best one-variable model

BCUTc-1l showed good correlation with the PDE4D inhibition. The model is shown below (Equation 9):

$$pIC_{50} = 17.4150\ (\pm 3.2812)\ BCUTc\text{-}1l + 11.7258\ (\pm 1.0782) \tag{9}$$

$n = 46$, $R^2 = 0.3903$, $R^2_{adj} = 0.3765$, SE $= 0.6082$, $F = 28.1700$

The best two-variable model

WNSA-3 was added into the Equation (9). The new equation showed great improvement in R^2. The model is shown below (Equation 10):

$$pIC_{50} = 18.2385\ (\pm 3.0027)\ BCUTc\text{-}1l - 0.0326\ (\pm 0.0103)$$
$$WNSA\text{-}3 + 10.8984\ (\pm 1.0174) \tag{10}$$

$n = 46$, $R^2 = 0.5048$, $R^2_{adj} = 0.4818$, SE $= 0.5544$, $F = 21.9180$

The best three-variable model

Regression analysis further incorporated nAtomP into Equation 10 and resulting in a new model with three descriptors. The best three-variable model is shown below (Equation 11):

$$pIC_{50} = 18.8576\ (\pm 2.7781)\ BCUTc\text{-}1l - 0.0443\ (\pm 0.0103)$$
$$WNSA\text{-}3 + 0.1121\ (\pm 0.0384)\ nAtomP + 8.4597\ (\pm 1.2563) \tag{11}$$

$n = 46$, $R^2 = 0.5884$, $R^2_{adj} = 0.5590$, SE $= 0.5115$, $F = 20.0130$

The best four-variable model

The four-variable model is formed by adding TPSA descriptor as correlating variable into Equation 11. The best four-variable model is shown below (Equation 12):

Table 6: Summary of statistical parameters of QSAR models for PDE4D inhibition

Model No.	R^2	R^2_{adj}	SE	F
Equation 9	0.3903	0.3765	0.6082	28.170
Equation 10	0.5048	0.4818	0.5544	21.918
Equation 11	0.5884	0.5590	0.5115	20.013
Equation 12	0.6660	0.6331	0.4665	20.411
Equation 13	0.7237	0.6892	0.4294	20.951
Equation 14	0.7720	0.7428	0.3864	26.412

QSAR: Quantitative structure–activity relationship, PDE4D: Phosphodiesterase 4D

$$pIC_{50} = 11.9412\ (\pm 3.3862)\ BCUTc\text{-}1l - 0.0717\ (\pm 0.0130)$$
$$WNSA\text{-}3 + 0.1424\ (\pm 0.0364)\ nAtomP - 0.0063\ (\pm 0.0020)$$
$$TPSA + 5.5665\ (\pm 1.4819) \tag{12}$$

$n = 46$, $R^2 = 0.6660$, $R^2_{adj} = 0.6331$, SE $= 0.4665$, $F = 20.4110$

The best five-variable model

Addition of C1SP3 into Equation 12 showed slight improvement in R^2 of equation. The five-variable model is shown below (Equation 13):

$$pIC_{50} = 10.2531\ (\pm 3.1709)\ BCUTc\text{-}1l - 0.0740\ (\pm 0.0120)$$
$$WNSA\text{-}3 + 0.1315\ (\pm 0.0337)\ nAtomP - 0.0079\ (\pm 0.0020)$$
$$TPSA - 0.1949\ (\pm 0.0673)\ C1SP3 + 6.0952\ (\pm 1.3762) \tag{13}$$

$n = 46$, $R^2 = 0.7237$, $R^2_{adj} = 0.6892$, SE $= 0.4294$, $F = 20.9510$

Addition of further descriptors did not improve the statistical parameters significantly, thus Equation 13 was selected as the optimum model for PDE4D inhibition. Analysis of residuals led to identification of molecule entry 8 as outlier. Thus, entry 8 was deleted from the training set to improve the regression. The best five-variable model for PDE4D inhibition is shown below (Equation 14), and the statistical parameters, correlation matrix of descriptors, and the actual and predicted activity are shown in Tables 6-8, respectively:

$$pIC_{50} = 10.5864\ (\pm 2.8549)\ BCUTc\text{-}1l - 0.0775\ (\pm 0.0108)$$
$$WNSA\text{-}3 + 0.1259\ (\pm 0.0304)\ nAtomP - 0.0078\ (\pm 0.0018)$$
$$TPSA - 0.1736\ (\pm 0.0609)\ C1SP3 + 6.0765\ (\pm 1.2383) \tag{14}$$

$n = 45$, $R^2 = 0.7720$, $R^2_{adj} = 0.7428$, SE $= 0.3864$, $F = 26.4120$

The best QSAR model for PDE4D inhibition consists of five descriptors with R^2 of 0.7720 (Equation 14) [Figure 2]. These five descriptors explain 77% of variation in the PDE4D inhibitory activity. Q^2 and R^2_{pred} of Equation 14 are 0.6798 and 0.6653, respectively. This suggests good predictive power of Equation 14. Five descriptors which contribute to the PDE4D inhibitory activity are BCUT-1l (descriptor related to intermolecular interaction), WNSA-3 (surface weighted charged partial negative charged surface area), nAtomP (number of atoms in the largest pi system), TPSA, and C1SP3 (singly bound carbon bound to another carbon).

The first descriptor that contributed to PDE4D inhibition is BCUTc-1l. BCUTc-1l is eigenvalue-based descriptor which accounts for partial charge and connectivity of atoms within the compound. BCUTc-1l utilized method of matrices, in

Table 7: Correlation matrix of descriptors present in the best QSAR model 14

Parameter	pIC_{50}	BCUTc-1l	WNSA-3	nAtomP	TPSA	C1SP3
pIC_{50}	1.0000					
BCUTc-1l	0.6430	1.0000				
WNSA-3	−0.3310	0.0917	1.0000			
nAtomP	0.0874	−0.0349	0.3661			
TPSA	−0.2937	−0.5871	−0.5811	−0.0229		
C1SP3	−0.2056	0.0302	0.1300	−0.1201	−0.2764	1.0000

QSAR: Quantitative structure–activity relationship

Table 8: Observed and predicted along with the residual obtained using QSAR model 14

Entry	Observed value	Predicted value	Residual
1	5.7212	5.4378	0.2834
2	5.4685	5.1170	0.3516
3	5.6778	5.4493	0.2285
4	5.1192	5.6055	−0.4864
5	5.8239	6.1295	−0.3056
6	5.8239	6.1590	−0.3351
7	5.0969	4.5851	0.5118
8	5.6198	5.6553	−0.0355
9	5.8861	5.6648	0.2213
10	6.0044	5.6693	0.3351
11	4.9208	5.3568	−0.4360
12	4.8239	5.3027	−0.4787
13	5.5229	5.0245	0.4984
14	5.5528	5.5823	−0.0294
15	5.8239	5.3259	0.4980
16	5.6990	5.5490	0.1500
17	5.8861	5.8353	0.0508
18	6.1192	5.6067	0.5125
19	4.9586	5.2244	−0.2657
21	5.0044	5.3255	−0.3211
22	5.3188	5.3650	−0.0463
23	5.3188	5.1604	0.1583
24	5.2757	5.1130	0.1627
25	5.7959	5.4753	0.3205
26	5.8239	5.9394	−0.1155
27	5.7696	6.2801	−0.5106
28	5.5376	5.4282	0.1094
29	5.5086	5.1708	0.3378
30	5.6383	4.3790	1.2593
33	5.4461	6.0458	−0.5997
34	6.4377	6.4699	−0.0322
36	5.8271	5.7985	0.0286
37	5.9278	5.9274	0.0003
38	5.2510	5.9197	−0.6687
39	4.6525	4.4041	0.2484
40	5.6763	5.3918	0.2845
41	6.1385	5.8930	0.2454
43	6.0660	6.0487	0.0173
44	6.1391	6.0796	0.0595
45	5.6444	6.0667	−0.4224
47	6.6003	6.7496	−0.1493
48	6.6840	6.6371	0.0470
49	6.6596	6.3669	0.2927
50	6.0526	6.6354	−0.5828

(Contd...)

Table 8: *(Continued)*

Entry	Observed value	Predicted value	Residual
51	7.6990	6.9869	0.7121
52	6.5719	6.9094	−0.3376
53	6.5719	6.6878	−0.1159
54	6.1669	6.2195	−0.0526
55	6.6716	6.8013	−0.1297
56	7.8861	7.4287	0.4573
57	8.1549	7.1547	1.0002
58	6.8794	7.2807	−0.4013
59	7.2007	6.8936	0.3071
60	6.7959	8.2388	−1.4429
62	6.2218	6.1444	0.0775

Entry 8 was identified as outlier and was deleted from training set whereas entry 61 was identified as outlier and deleted from test set

which the diagonal matrix elements are based on computed physicochemical parameters related to a partial charge of the compound.[26] BCUTc-1l has the highest contribution among all descriptors in PDE4D inhibition. Positive coefficient of BCUTc-1l shows that increase in magnitude of BCUTc-1l of compound will increase its PDE4D inhibitory activity.

WNSA-3 is surface-weighted charged partial negative charged surface area that combines surface area and partial charge information. Formula for WNSA-3 is shown below (Equations 17 and 18):[21]

$$\text{WNSA-3} = \frac{\text{PNSA}_3 \times \text{SASA}}{1000} \qquad (17)$$

$$\text{PNSA}_3 = \sum_{a^-} q_a^- \, \text{SA}_a^- \qquad (18)$$

PNSA_3 is atomic charged weighted positive surface area whereas SASA is total molecular solvent-accessible surface area. It is sum of the product of atomic solvent-accessible surface area by partial charge overall negatively charged atoms.[27] WNSA-3 has a negative correlation with PDE4D inhibition activity. nAtomP is a number of atoms in largest pi system of the molecule. Aromatic ring is the largest pi system in 2-arylpyridine and s-triazine system. The positive coefficient indicates that the higher the number of atoms involved in the aromatic pi system, the better the PDE4D inhibitory activity. nAtomP of entry 51 is 22, which is higher than entry 44 with nAtomP of 13 accordingly; thus, PDE4D inhibitory activity of entry 51 is higher than entry 13.

TPSA is the fourth descriptor in terms of its contribution to the PDE4D inhibitory activity. Similar to PDE4B model, TPSA of the compounds contributes negatively to its PDE4D inhibitory activity. Both TPSA and WNSA-3 are descriptors related to surface area and charge. The correlation coefficient of TPSA and WNSA-3 is −0.581118. Incorporation of TPSA into equation increases R^2 by 0.0776, from 0.5884 to 0.6660. Hence, it is worthwhile to include both TPSA and WNSA-3 in PDE4D inhibition model. The last descriptor is C1SP3; it is the number of singly bound carbon atom bound to another carbon. Singly bound carbon atom is sp³ hybridisation,

bond to another atom and two non-carbon atoms such as hydrogen or oxygen. Equation 14 shows that increasing number of C1SP3 atoms will decrease the inhibitory activity of compound.

According to the model 8 and 14, TPSA has positive correlation with PDE4B and PDE4D inhibitory activities of compound. Hence, TPSA has insignificant role in determining selectivity of the compound toward PDE4B inhibition. The number of C1SP1 atoms within compound is positively correlated with the PDE4B inhibitory activity of compound whereas a number of C1SP3 atoms is negatively correlated with PDE4D inhibition. A new compound is designed based on model 8 and 14 [Figure 3] which contained favorable descriptors for inhibition of PDE4B.

In the new compound, introduction of methyl group on the thiophenyl ring at position R$_3$ of compound will increase C1SP3 and ATSm4. Since ATSm4 is positively correlated with inhibition of PDE4B and C1SP3 is inversely correlated with

PDE4D inhibition, selectivity of compound toward PDE4B will be increased.

Introduction of methoxy group on thiophenyl substituent will increase electronegativity of the compound due to the presence of extra oxygen atom. Relative negative charge within the compound will decrease and RNCS of the compound will increase. Since RNCS is positively correlated with inhibition of PDE4B; thus, substitution is favorable for inhibition of PDE4B.

Cross-validation

The Equations 8 and 14 were subjected to internal validation and external validation. In external validation for PDE4B inhibition model, two outliers (entry 30 and 59) with high standard residual values were deleted from test set [Table 9]. In external validation for PDE4D inhibition model, one outlier (entry 61) was deleted from test set.

Internal validation

Internal validation of model 8 and model 14 was performed using LOO method. The LOO method consists of developing a number of models omitting one compound at the time after developing each model.[28] Model 8 has Q^2 value of 0.5589 and R^2-Q^2 value of 0.1577. Q^2 higher than 0.5 and R^2-Q^2 smaller than 0.3 suggests that model 8 has good predictive ability. However, Q^2 value higher or equal than 0.9 is required for an excellent model.[28] The best QSAR model for PDE4B inhibition (Equation 8) has F value of 14.814 which indicates the overall significance of the model. Standard error of Equation 8 is 0.3864. High F value and small standard error explains small variance due to error and shows the excellent reliability of the model.

Q^2 and R^2-Q^2 of model 14 are 0.6798 and 0.0922, respectively. F value and standard error of model 14 are 26.412 and 0.3864, respectively. It has a higher F and lower standard error when compared to model 8. Therefore, model 14 has greater predictive power compared to model 8. PRESS value for model 14 is lower than model 8. The lower the PRESS value, the better the fit of the model to the new training set obtained by randomly removing one compound.

External validation

Test set is used to validate the external validity of model 8 and 14. Model 8 is a reliable model because it has R^2_{pred} of 0.7645. For model 8, entry 12 has highest residual value, which is 0.7881. Observed activity of entry 12 is 5.5528, whereas predicted activity of entry 12 using Equation 8 is 6.3409. Model 14 has R^2_{pred} of 0.6653 which is smaller than R^2_{pred} of model 8. Model 14 has less predictive power than model 8. However, model 14 is considered as a reliable model because R^2_{pred} is higher than 0.6.
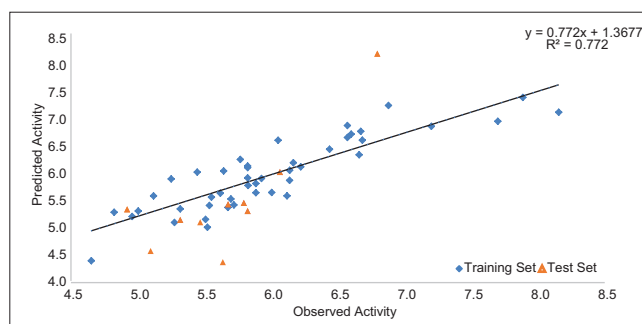
Figure 2: Predicted versus observed activity of model 14
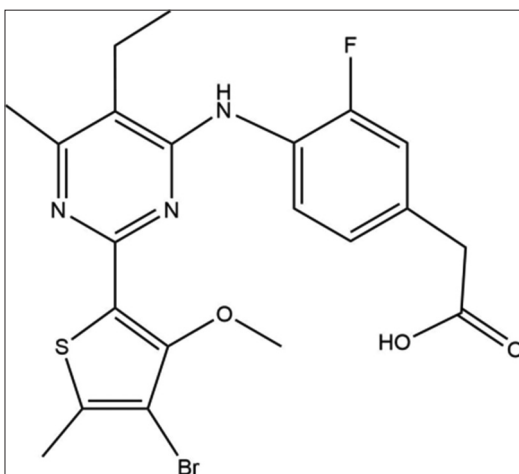
Figure 3: New compound (PCS-I) designed based on quantitative structure–activity relationship model 8 and 14

Table 9: Cross-validation parameter for model

Model No.	N$_{test}$	PRESS	Q^2	RMSECV	Q^2_{pred}	F	SE
8	10	12.0250	0.5589	0.4954	0.7645	14.814	0.4341
14	10	8.1770	0.6798	0.4263	0.6653	26.412	0.3864

SE: Standard error

CONCLUSION

In QSAR model for PDE4B inhibition, R^2 value of model increases when a number of valid descriptors included in the model increases. The optimum number of descriptors in QSAR model for PDE4B inhibition is seven. R^2 of the best seven-variable model for PDE4B inhibition is 0.7166. The results indicate that ATSm4, Wlambda3.unity, C1SP1, RNCS, TPSA, asa_ASA_P_pH_7.4, and maximal projection radius are important in determining the PDE4B inhibition of the compound. ATSm4, C1SP1, RNCS, asa_ASA_P_pH_7.4, and maximal projection radius have a positive correlation with PDE4B inhibitory activity whereas Wlambda3.unity and TPSA are negatively correlated with PDE4B inhibitory activity. Among seven descriptors, C1SP1 has the highest contribution to the PDE4B inhibition whereas TPSA has a lowest contribution to the PDE4B inhibition.

In QSAR model for PDE4D inhibition, the optimum number of descriptors is five. BCUT-1l, WNSA-3, nAtomP, TPSA, and C1SP3 are vital structural features in determining the PDE4D inhibition of the compound. BCUTc-1l and nAtomP have positive correlation with the PDE4D inhibition, while WNSA-3, TPSA, and C1SP3 are negatively correlated with the PDE4D inhibition. Contribution of BCUTc-1l to PDE4D inhibition is highest whereas contribution of TPSA to PDE4D is lowest.

Model 8 for PDE4B inhibition has R^2_{pred} of 0.7645, whereas model 14 for PDE4D has R^2_{pred} of 0.6653. Both models 8 and 14 have acceptable external validity because R^2_{pred} is higher than 0.6.

The information obtained from these models was used to design a new compound PCS-I with higher PDE4B selectivity. PDE4B selectivity of new compound is introduced by increasing ATSm4, decreasing C1SP3, and decreasing RNCS.

REFERENCES

1. (a) Durham AL, Caramori G, Chung KF, Adcock IM. Targeted anti-inflammatory therapeutics in asthma and chronic obstructive lung disease. Transl Res 2016;167:192-203. (b) Pelaia G, Muzzio CC, Vatrella A, Maselli R, Magnoni MS, Rizzi A, *et al*. Pharmacological basis and scientific rationale underlying the targeted use of inhaled corticosteroid/long-acting β2-adrenergic agonist combinations in chronic obstructive pulmonary disease treatment. Expert Opin Pharmacother 2015;16:2009-21. (c) Garvey C. Recent updates in chronic obstructive pulmonary disease. Postgrad Med 2016;128:231-8.

2. Montuschi P. Pharmacological treatment of chronic obstructive pulmonary disease. Int J Chron Obstruct Pulmon Dis 2006;1:409-23.

3. Ito K, Ito M, Elliott WM, Cosio B, Caramori G, Kon OM, *et al*. Decreased histone deacetylase activity in chronic obstructive pulmonary disease. N Engl J Med 2005;352:1967-76.

4. Marwick JA, Caramori G, Casolari P, Mazzoni F, Kirkham PA, Adcock IM, *et al*. A role for phosphoinositol 3-kinase delta in the impairment of glucocorticoid responsiveness in patients with chronic obstructive pulmonary disease. J Allergy Clin Immunol 2010;125:1146-53.

5. (a) Press NJ, Banner KH. PDE4 inhibitors-a review of the current field. Prog Med Chem 2009;47:37-74. (b) Burgin AB, Magnusson OT, Singh J, Witte P, Staker BL, Bjornsson JM, *et al*. Design of phosphodiesterase 4D (PDE4D) allosteric modulators

6. (a) Barnette MS. Phosphodiesterase 4 (PDE4) inhibitors in asthma and chronic obstructive pulmonary disease (COPD). Prog Drug Res 1999;53:193-229. (b) Diamant Z, Spina D. PDE4-inhibitors: A novel, targeted therapy for obstructive airways disease. Pulm Pharmacol Ther 2011;24:353-60. (c) Torphy TJ. Phosphodiesterase isozymes: Molecular targets for novel antiasthma agents. Am J Respir Crit Care Med 1998;157:351-70.

7. Garnock-Jones KP. Roflumilast: A review in COPD. Drugs 2015;75:1645-56.

8. Beghè B, Rabe KF, Fabbri LM. Phosphodiesterase-4 inhibitor therapy for lung diseases. Am J Respir Crit Care Med 2013;188:271-8.

9. (a) Pérez-Torres S, Miró X, Palacios JM, Cortés R, Puigdoménech P, Mengod G, *et al*. Phosphodiesterase Type 4 isozymes expression in human brain examined by *in situ* hybridization histochemistry and[3H]rolipram binding autoradiography. Comparison with monkey and rat brain. J Chem Neuroanat 2000;20:349-74. (b) Lamontagne S, Meadows E, Luk P, Normandin D, Muise E, Boulet L, *et al*. Localization of phosphodiesterase-4 isoforms in the medulla and nodose ganglion of the squirrel monkey. Brain Res 2001;920:84-96.

10. Robichaud A, Stamatiou PB, Jin SL, Lachance N, MacDonald D, Laliberté F, *et al*. Deletion of phosphodiesterase 4D in mice shortens alpha(2)-adrenoceptor-mediated anesthesia, a behavioral correlate of emesis. J Clin Invest 2002;110:1045-52.

11. (a) Naganuma K, Omura A, Maekawara N, Saitoh M, Ohkawa N, Kubota T, *et al*. Discovery of selective PDE4B inhibitors. Bioorg Med Chem Lett 2009;19:3174-6. (b) Jin SL, Goya S, Nakae S, Wang D, Bruss M, Hou C, *et al*. Phosphodiesterase 4B is essential for T(H)2-cell function and development of airway hyperresponsiveness in allergic asthma. J Allergy Clin Immunol 2010;126:1252-9e12.

12. Hagen TJ, Mo X, Burgin AB, Fox D 3rd, Zhang Z, Gurney ME, *et al*. Discovery of triazines as selective PDE4B versus PDE4D inhibitors. Bioorg Med Chem Lett 2014;24:4031-4.

13. (a) Kolb P, Phan K, Gao ZG, Marko AC, Sali A, Jacobson KA, *et al*. Limits of ligand selectivity from docking to models: *In silico* screening for A(1) adenosine receptor antagonists. PLoS One 2012;7:e49910. (b) Wang Z, Li Y, Ai C, Wang Y. *In silico* prediction of estrogen receptor subtype binding affinity and selectivity using statistical methods and molecular docking with 2-arylnaphthalenes and 2-arylquinolines. Int J Mol Sci 2010;11:3434-58. (c) Giełdoń A, Kaźmierkiewicz R, Slusarz R, Pasenkiewicz-Gierula M, Ciarkowski J. Molecular dynamics study of 4-OH-phenylacetyl- D-Y(Me)FQNRPR-NH2 selectivity to V1a receptor. J Mol Model 2003;9:372-8. (d) Zeng J, Li W, Zhao Y, Liu G, Tang Y, Jiang H, *et al*. Insights into ligand selectivity in estrogen receptor isoforms: Molecular dynamics simulations and binding free energy calculations. J Phys Chem B 2008;112:2719-26.

14. Bourguet W, Ruff M, Chambon P, Gronemeyer H, Moras D. ACD/ChemSketch. Version. 1. Toronto, Canada: Advanced Chemistry Development, Inc.; 2016.

15. Sushko I, Novotarskyi S, Körner R, Pandey AK, Rupp M, Teetz W, *et al*. Online chemical modeling environment (OCHEM): Web platform for data storage, model development and publishing of chemical information. J Comput Aided Mol Des 2011;25:533-54.

16. Novotarskyi S. Molecule Preprocessing. Available from: http://docs.ochem.eu/display/MAN/Molecule+preprocessing. [Last accessed on 2016 Aug 23].

17. MATLAB R2016b. The MathWorks, Inc. Natick, Massachusetts, United States: The MathWorks, Inc.; 2016.

18. STATISTICA (Data Analysis Software System), Stat Soft, Inc.; 2011. p. 10.

19. Veerasamy HR, Jain A, Sivadasan S, Varghese CP, Agrawal RK.

Validation of QSAR models - Strategies and importance. Int J Drug Discov 2011;2:511-9.

20. Tropsha A. Best Practices for QSAR Model Development, Validation, and Exploitation. Vol. 29. Weinheim: WILEY-VCH Verlag GmbH & Co. KGaA; 2010.

21. Todeschini VC. Handbook of Molecular Descriptors. Vol. 11. Weinheim and New York: Wiley-VCH; 2008. p. 688.

22. Todeschini R, Provenzani R, Marengo E. Weighted holistic invariant molecular descriptors. Part 2. Theory development and applications on modeling physicochemical properties of polyaromatic hydrocarbons. Chemom Intell Lab 1995;27:227-9.

23. Todeschini ML, Marengo E. New molecular descriptors for 2D and 3D structures theory. J. Chemometrics 1994;8:263-72.

24. Prasanna S, Doerksen RJ. Topological polar surface area: A useful descriptor in 2D-QSAR. Curr Med Chem 2009;16:21-41.

25. (a) Strazielle N, Ghersi-Egea JF. Factors affecting delivery of antiviral drugs to the brain. J Med Virol 2005;15:105-33. (b) Li S, He H, Parthiban LJ, Yin H, Serajuddin AT. IV-IVC considerations in the development of immediate-release oral dosage form. J Pharm Sci 2005; 94:1396-417.

26. Mason JS, Beno BR. Library design using BCUT chemistry-space descriptors and multiple four-point pharmacophore fingerprints: Simultaneous optimization and structure-based diversity. J Mol Graph Model 2000;18:438-51.

27. Todeschini VC. Molecular Descriptors for Chemoinformatics. Vol. 41. Hoboken, NJ: John Wiley & Sons; 2009.

28. Singh J, Shaik B, Singh S, Agrawal VK, Khadikar PV, Deeb O, *et al*. Comparative QSAR study on para-substituted aromatic sulphonamides as CAII inhibitors: Information versus topological (distance-based and connectivity) indices. Chem Biol Drug Des 2008;71:244-59.